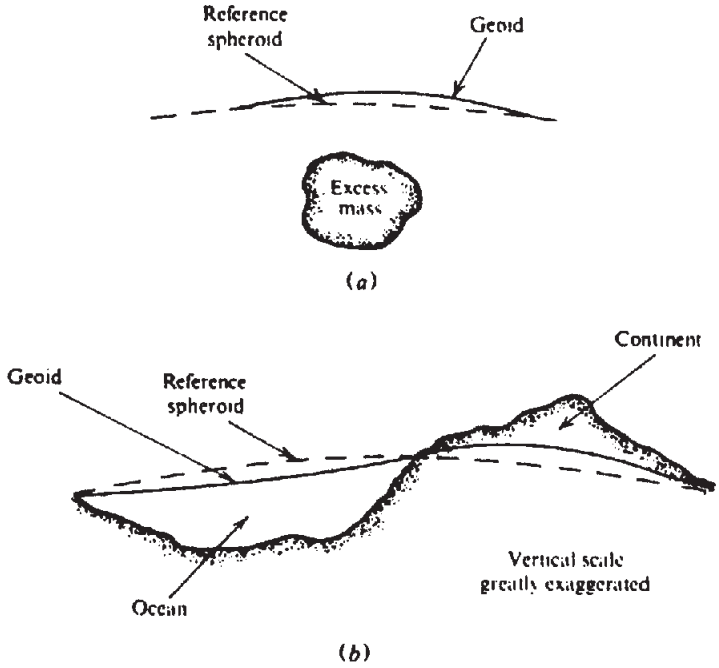

Figure 2.2. Comparison of reference spheroid and geoid. (a) Warping of the geoid by a local mass. (b) Large-scale warping.

the geoid to be warped upward under the continents because of attracting material above, and downward over the ocean basins because of the low density of water (Figure 2.2b). However, deviations from the spheroid do not correlate with the continents nor with the lithospheric plates, suggesting that density differences exist below the lithosphere. The deviations between the two surfaces (Kahn, 1983) are as much as 100 m.

2.3.2. Gravity Reduction

(a) General. Gravity readings are generally influenced by the five factors listed in Section 2.3.1a, hence we must make corrections to reduce gravity readings to the values they would have on a datum equipotential surface such as the geoid (or a surface everywhere parallel to it).

(b) Latitude correction. Both the rotation of the Earth and its equatorial bulge produce an increase of gravity with latitude. The centrifugal acceleration due to the rotating Earth is maximum at the equator and zero at the poles; it opposes the gravitational acceleration, while the polar flattening increases gravity at the poles by making the geoid closer to the Earth's center of mass. The latter effect is counteracted partly by the increased attracting mass at the equator. A *latitude correction* Δg_L is obtained by differentiating Equation (2.20):

$$\Delta g_L/\Delta s = (1/R_e)\,\Delta g_t/\Delta\phi$$

$$= 0.811 \sin 2\phi \text{ mGal/km} \quad (2.21a)$$

$$= 1.305 \sin 2\phi \text{ mGal/mile} \quad (2.21b)$$

where Δs = N–S horizontal distance = $R_e\,\Delta\phi$ and R_e is the radius of the Earth ($\approx$ 6368 km). The correction is a maximum at latitude 45° where it amounts to 0.01 mGal/(13 m) and it is zero at the equator and poles. The correction is added to g as we move toward the equator.

(c) Free-air correction. Since gravity varies inversely with the square of distance, it is necessary to correct for changes in elevation between stations to reduce field readings to a datum surface. The *free air correction* does not take account of the material between the station and the datum plane. It is obtained by differentiating the scalar equation equivalent to Equation (2.2b); the result is (dropping the minus sign)

$$\Delta g_{FA}/\Delta R = 2\gamma M_e/R_e^3 = 2g/R_e$$

$$= 0.3086 \text{ mGal/m} \quad (2.22a)$$

$$= 0.09406 \text{ mGal/ft} \quad (2.22b)$$

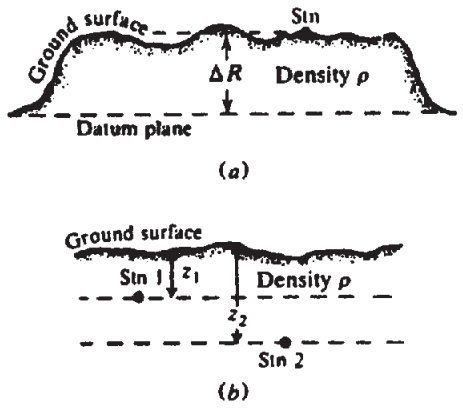

Figure 2.3. Bouguer correction. (a) Station on a broad plateau. (b) Underground stations.

at 45° latitude. The free-air correction is added to the field reading when the station is above the datum plane and subtracted when below it.

To make latitude and free-air corrections, station position must be known precisely. For an accuracy of 0.01 mGal, the usual accuracy of the gravimeter, N–S location (at 45° latitude) must be known to within 13 m (40 ft) and elevation to 3 cm (1 in.).

(d) Bouguer correction. The *Bouguer correction* accounts for the attraction of material between the station and datum plane that was ignored in the free-air calculation. If the station were centrally located on a plateau of large horizontal extent and uniform thickness and density (Fig. 2.3a), the gravity reading would be increased by the attraction of this slab between the station and the datum. The Bouguer correction is given by

$$\Delta g_B/\Delta R = 2\pi\gamma\rho$$

$$= 0.04192\rho \text{ mGal/m} \quad (2.23a)$$

$$= 0.01278\rho \text{ mGal/ft} \quad (2.23b)$$

where ρ is the slab density in grams per cubic centimeter [see Eq. (2.57)]. If we assume an average density for crustal rocks of 2.67 g/cm^3, the numerical value is

$$\Delta g_B/\Delta R = 0.112 \text{ mGal/m} \quad (2.24a)$$

$$= 0.0341 \text{ mGal/ft} \quad (2.24b)$$

The Bouguer correction is applied in the opposite sense to free air, that is, it is subtracted when the station is above the datum and vice versa.

When gravity measurements are made at underground stations, as in Figure 2.3b, the slab between stations at depths z_1 and z_2 exerts an attraction downward on station 1 and upward on 2. Thus the difference in gravity between them is $4\pi\gamma\rho(z_2 - z_1)$ mGal, that is, the Bouguer correction is doubled.

The Bouguer and free-air corrections are often combined into an *elevation correction.* From Equations (2.22) and (2.23) the result is

$$\Delta g_E/\Delta R = \Delta g_{FA}/\Delta R - \Delta g_B/\Delta R$$

$$= (0.3086 - 0.0419\rho) \text{ mGal/m} \quad (2.25a)$$

$$= (0.0941 - 0.0128\rho) \text{ mGal/ft} \quad (2.25b)$$

The elevation correction is applied in the same way as the free-air correction.

Two assumptions were made in deriving the Bouguer correction: (1) The slab is of uniform density and (2) it is of infinite horizontal extent; neither is really valid. To modify the first, one needs considerable knowledge of local rock types and densities. The second is taken care of in the next reduction.

(e) Terrain correction. The terrain correction allows for surface irregularities in the vicinity of the station. Hills above the elevation of the gravity station exert an upward pull on the gravimeter, whereas valleys (lack of material) below it fail to pull downward on it. Thus both types of topographic undulations affect gravity measurements in the same sense and the *terrain correction* is added to the station reading.

There are several methods for calculating terrain corrections, all of which require detailed knowledge of relief near the station and a good topographical map (contour interval ~ 10 m or 50 ft or smaller) extending considerably beyond the survey area. The usual procedure is to divide the area into compartments and compare the elevation within each compartment with the station elevation. This can be done by outlining the compartments on a transparent sheet overlying a topographic map. The most common template used concentric circles and radial lines, making sectors whose areas increased with distance from the station. The gravity effect of a single sector was calculated from the following for-

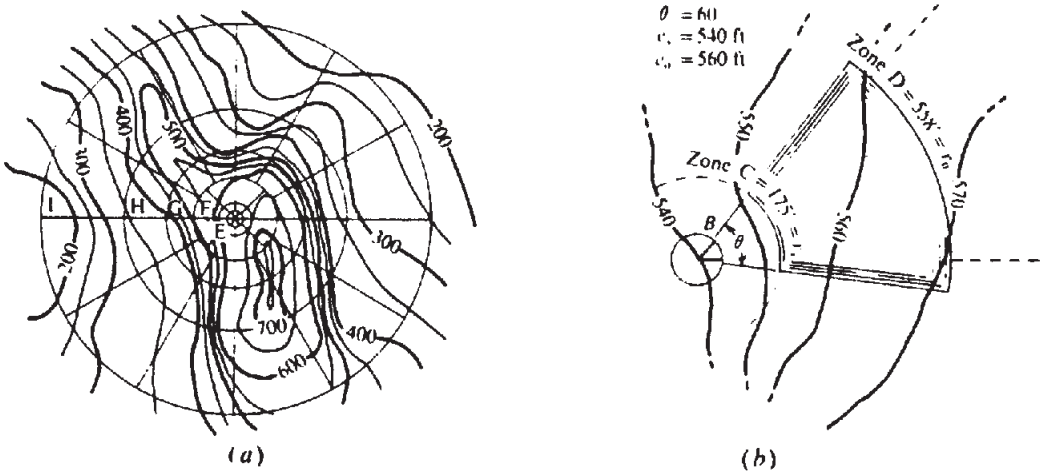

Figure 2.4. Use of terrain chart with topographic map. (a) Terrain chart overlying map. (b) Enlarged view of a single zone.

mula [Eq. (2.58)]:

$$\delta g_T(r,\theta) = \gamma\rho\theta\left\{(r_o - r_i) + \left(r_i^2 + \Delta z^2\right)^{1/2} - \left(r_o^2 + \Delta z^2\right)^{1/2}\right\} \quad (2.26)$$

where θ is the sector angle (radians), $\Delta z = |z_s - z_a|$, z_s is the station elevation, z_a is the average elevation in the sector, and r_o and r_i are the outer and inner sector radii. The terrain correction Δg_T is the sum of the contributions of all sectors:

$$\Delta g_T = \sum_r \sum_\theta \delta g_T(r,\theta) \quad (2.27)$$

The use of a terrain chart of this type is illustrated in Figure 2.4. The transparent template is placed over the topographic map with the center of the circles at the gravity station. The average elevation within a single compartment is estimated from the contours within it and subtracted from the known station elevation. The difference is Δz in Equation (2.26), from which the contribution to Δg_T is calculated for the compartment. Tables of terrain corrections such as Table 2.1 facilitated this operation. [Hammer (1982) gives corrections for subdivisions of the inner zones required in microgravity surveys for engineering and archaeological surveys.] Note that there was no provision for relief within 2 m of the station, that is, it has to be flat for a 2 m distance from the station. It can be seen from Table 2.1 that the correction is small if $r > 20z$, r being the average distance from the compartment to the station.

Other methods for segmenting the topographic map occasionally were applied; for instance, when contours were practically linear, there was no advantage in using circular sectors. An alternative scheme used elementary areas so proportioned that the gravity effect of each was the same regardless of distance.

Terrain corrections for outer zones are often made on a computer using elevations on a regular grid (Krohn, 1976). Regardless of the approach, the topographic reduction is a slow and tedious task. Furthermore, in areas of steep and erratic slopes, it usually is not very accurate, particularly for relief in the vicinity of the station itself. At the edge of a steep cliff or gorge, the terrain correction is almost inevitably in error. A better solution is to move the gravity station away from sharp relief features if this is possible.

Bouguer anomalies (§2.3.2h) for marine surface and airborne surveys require a different terrain correction from that discussed earlier. The Bouguer correction is calculated (for marine data) as if the water depth were everywhere constant, and hence it is discontinuous over abrupt elevation changes. The terrain correction is made discontinuous to compensate for the Bouguer correction discontinuities. To the left of a two-dimensional vertical step in the sea floor (Fig. 2.5), the terrain correction is positive due to the deeper water on the right (analogous to a nearby valley in land work), and it is negative to the right of the step.

(f) Earth-tide correction. Instruments for measuring gravity are sensitive enough to record the changes in g caused by movement of the Sun and Moon, changes that depend on latitude and time. Their range is about 0.3 mGal. Figure 2.6 shows calculated and measured tidal variations for a stationary gravimeter.

The correction can be calculated from knowledge of the locations of the Sun and Moon. However, because the variation is smooth and relatively slow,

Table 2.1. *Terrain corrections.*

Zone B 4 sectors 6.56′ – 54.6′		Zone C 6 sectors 54.6′ – 175′		Zone D 6 sectors 175′ – 558′		Zone E 8 sectors 558′ – 1280′		Zone F 8 sectors 1280′ – 2936′		Zone G 12 sectors 2936′ – 5018′		Zone H 12 sectors 5018′ – 8578′		Zone I 12 sectors 8578′ – 14612′	
$\pm z$	dg_T	$\pm z$	dg_T	$\pm z$	dg_T	$\pm z$	dg_T	$\pm z$	dg_T	$\pm z$	dg_T	$\pm z$	dg_T	$\pm z$	dg_T
0.0 – 1.1	0.00000	0.0 – 4.3	0.00000	0.0 – 7.7	0.00000	0 – 18	0.00000	0 – 27	0.00000	0 – 58	0.00000	0 – 75	0.00000	0 – 99	0.00000
1.1 – 1.9	0.00133	4.3 – 7.5	0.00133	7.7 – 13.4	0.00133	18 – 30	0.00133	27 – 46	0.0133	58 – 100	0.00133	75 – 131	0.00133	99 – 171	0.00133
1.9 – 2.5	0.00267	7.5 – 9.7	0.00267	13.4 – 17.3	0.00267	30 – 39	0.00267	46 – 60	0.00267	100 – 129	0.00267	131 – 169	0.00267	171 – 220	0.00267
2.5 – 2.9	0.0040	9.7 – 11.5	0.0040	17.3 – 20.5	0.0040	39 – 47	0.0040	60 – 71	0.0040	129 – 153	0.0040	169 – 200	0.0040	220 – 261	0.0040
2.9 – 3.4	0.0053	11.5 – 13.1	0.0053	20.5 – 23.2	0.0053	47 – 53	0.0053	71 – 80	0.0053	153 – 173	0.0053	200 – 226	0.0053	261 – 296	0.0053
3.4 – 3.7	0.0067	13.1 – 14.5	0.0067	23.2 – 25.7	0.0067	53 – 58	0.0067	80 – 88	0.0067	173 – 191	0.0067	226 – 250	0.0067	296 – 327	0.0067
3.7 – 7	0.0133	14.5 – 24	0.0133	25.7 – 43	0.0133	58 – 97	0.0133	88 – 146	0.0133	191 – 317	0.0133	250 – 414	0.0133	327 – 540	0.0133
7 – 9	0.0267	24 – 32	0.0267	43 – 56	0.0267	97 – 126	0.0267	146 – 189	0.0267	317 – 410	0.0267	414 – 535	0.0267	540 – 698	0.0267
9 – 12	0.040	32 – 39	0.040	56 – 66	0.040	126 – 148	0.040	189 – 224	0.040	410 – 486	0.040	535 – 633	0.040	698 – 827	0.040
12 – 14	0.053	39 – 45	0.053	66 – 76	0.053	148 – 170	0.053	224 – 255	0.053	486 – 552	0.053	633 – 719	0.053	827 – 938	0.053
14 – 16	0.067	45 – 51	0.067	76 – 84	0.067	170 – 189	0.067	255 – 282	0.067	552 – 611	0.067	719 – 796	0.067	938 – 1038	0.067
16 – 19	0.080	51 – 57	0.080	84 – 92	0.080	189 – 206	0.080	282 – 308	0.080	611 – 666	0.080	796 – 866	0.080	1038 – 1129	0.080
19 – 21	0.0935	57 – 63	0.0935	92 – 100	0.0935	206 – 222	0.0935	308 – 331	0.0935	666 – 716	0.0935	866 – 931	0.0935		
21 – 24	0.107	63 – 68	0.107	100 – 107	0.107	222 – 238	0.107	331 – 353	0.107	716 – 764	0.107	931 – 992	0.107		
24 – 27	0.120	68 – 74	0.120	107 – 114	0.120	238 – 252	0.120	353 – 374	0.120	764 – 809	0.120	992 – 1050	0.120		
27 – 30	0.133	74 – 80	0.133	114 – 120	0.133	252 – 266	0.133	374 – 394	0.133	809 – 852	0.133	1050 – 1105	0.133		
		80 – 86	0.147	120 – 127	0.147	266 – 280	0.147	394 – 413	0.147	852 – 894	0.147				
		86 – 91	0.160	127 – 133	0.160	280 – 293	0.160	413 – 431	0.160	894 – 933	0.160				
		91 – 97	0.174	133 – 140	0.174	293 – 306	0.174	431 – 449	0.174	933 – 972	0.174				
		97 – 104	0.187	140 – 146	0.187	306 – 318	0.187	449 – 466	0.187	972 – 1009	0.187				
		104 – 110	0.200	146 – 152	0.200	318 – 331	0.200	466 – 483	0.200	1009 – 1046	0.200				

Note: $dg_T = \theta\gamma\rho\{r_o - r_i + \sqrt{(r_i^2 + z^2)} - \sqrt{(r_o^2 + z^2)}\}$, r_i, r_o = inner, outer sector radii, $\gamma = 6.67 \times 10^{-8}$, dg_T in milligals, z, r_i, r_o in feet, and z = average sector elevation.
Source: From Hammer (1939), but based on average density $\rho = 2.67$ g/cm^3.

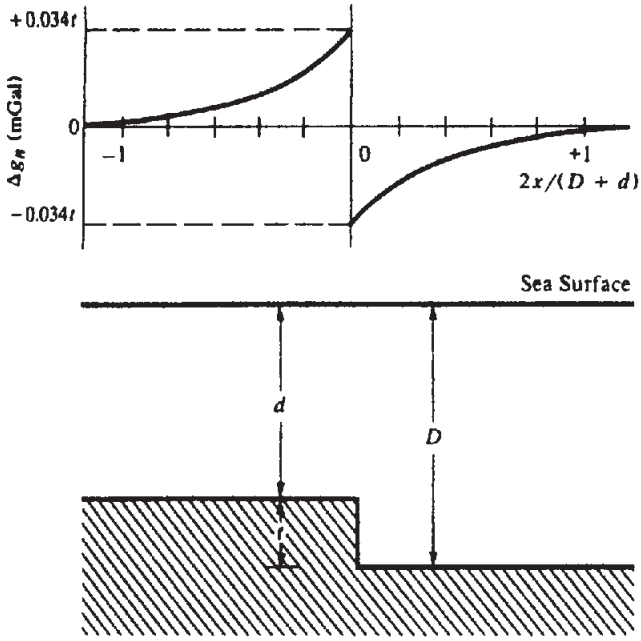

Figure 2.5. Marine terrain correction for vertical sea-floor step. ρ_w = 1.03, ρ_{rock} = 2.67, t = meters. (After Nettleton, 1971.)

usually it is included in the instrument drift correction (§2.5.2).

(g) Isostatic correction. The worldwide average of Bouguer anomalies on land near sea level is approximately zero. In regions of large elevation they are generally negative, while in oceanic regions mainly positive. These large-scale effects are due to density variations in the crust, indicating denser material beneath the ocean and less dense material in regions of elevated land.

In 1855, two hypotheses were put forward to account for the density variations. Airy proposed a crust of uniform density but variable thickness floating on a liquid substratum of higher density, whereas Pratt suggested a crust where the density varies with topography, being lower in mountain regions and higher beneath the oceans. Both hypotheses appear to be true to some extent. An *isostatic correction* occasionally is necessary in large-scale surveys to compensate for crustal variations.

(h) Bouguer and free-air anomalies. When all of the preceding corrections have been applied to the observed gravity reading, we obtain the value of the *Bouguer anomaly* g_B for the station:

$$g_B = g_{obs} - g_t + (\Delta g_L + \Delta g_{FA} - \Delta g_B + \Delta g_T) \tag{2.28}$$

where g_{obs} is the station reading, g_t is the theoretical gravity, Δg_L is the latitude correction, Δg_{FA} is the free-air correction, Δg_B is the Bouguer correction, and Δg_T is the terrain correction. The correction terms in Equation (2.28) correspond to a station south of the reference latitude (in the northern hemisphere) and above the datum. Sometimes, rather than the value from Equation (2.20), some particular station value in the survey area is used for g_t. Note that the signs of Δg_{FA} and Δg_B change when the station is below the datum plane.

Another quantity that is sometimes used (especially with marine data) is the *free-air anomaly*, the value of g_B when Δg_B (and often Δg_T) is omitted from Equation (2.28).

If the Earth had no lateral variations in density, after corrections for the preceding effects, gravity readings would be identical. The Bouguer and free-air anomalies result from lateral variations in density (see also Ervin, 1977).

2.3.3. Densities of Rocks and Minerals

The quantity to be determined in gravity exploration is local lateral variation in density. Generally density

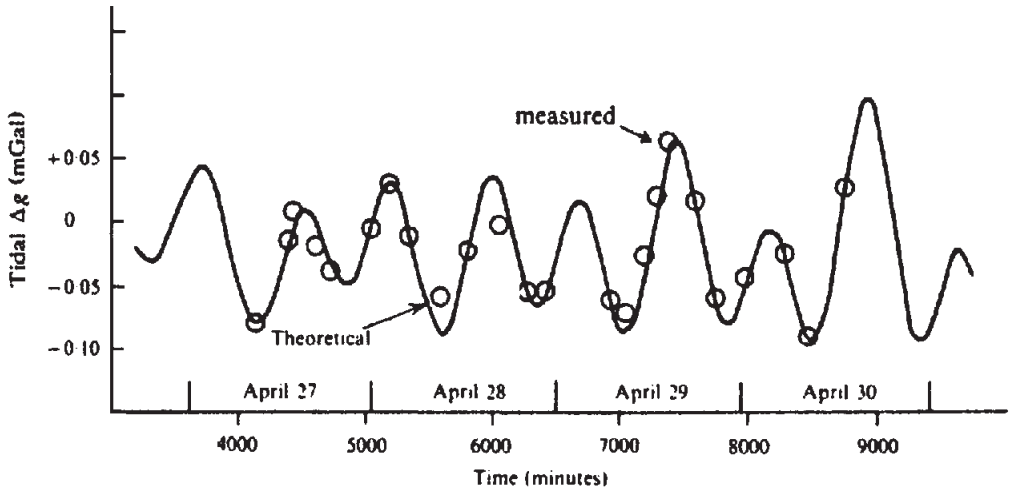

Figure 2.6. Earth-tide variations, Montreal, April 1969. Gravity readings have been corrected for instrument drift.

Table 2.2. *Densities.*

Rock type	Range (g/cm^3)	Average (g/cm^3)
Sediments (wet)		
Overburden		1.92
Soil	1.2 – 2.4	1.92
Clay	1.63 – 2.6	2.21
Gravel	1.7 – 2.4	2.0
Sand	1.7 – 2.3	2.0
Sandstone	1.61 – 2.76	2.35
Shale	1.77 – 3.2	2.40
Limestone	1.93 – 2.90	2.55
Dolomite	2.28 – 2.90	2.70
Sedimentary rocks (av.)		2.50
Igneous rocks		
Rhyolite	2.35 – 2.70	2.52
Andesite	2.4 – 2.8	2.61
Granite	2.50 – 2.81	2.64
Granodiorite	2.67 – 2.79	2.73
Porphyry	2.60 – 2.89	2.74
Quartz diorite	2.62 – 2.96	2.79
Diorite	2.72 – 2.99	2.85
Lavas	2.80 – 3.00	2.90
Diabase	2.50 – 3.20	2.91
Basalt	2.70 – 3.30	2.99
Gabbro	2.70 – 3.50	3.03
Peridotite	2.78 – 3.37	3.15
Acid igneous	2.30 – 3.11	2.61
Basic igneous	2.09 – 3.17	2.79
Metamorphic rocks		
Quartzite	2.5 – 2.70	2.60
Schists	2.39 – 2.9	2.64
Graywacke	2.6 – 2.7	2.65
Marble	2.6 – 2.9	2.75
Serpentine	2.4 – 3.10	2.78
Slate	2.7 – 2.9	2.79
Gneiss	2.59 – 3.0	2.80
Amphibolite	2.90 – 3.04	2.96
Eclogite	3.2 – 3.54	3.37
Metamorphic	2.4 – 3.1	2.74

Mineral	Range (g/cm^3)	Average (g/cm^3)
Metallic minerals		
Oxides, carbonates		
Bauxite	2.3 – 2.55	2.45
Limonite	3.5 – 4.0	3.78
Siderite	3.7 – 3.9	3.83
Rutile	4.18 – 4.3	4.25
Manganite	4.2 – 4.4	4.32
Chromite	4.3 – 4.6	4.36
Ilmenite	4.3 – 5.0	4.67
Pyrolusite	4.7 – 5.0	4.82
Magnetite	4.9 – 5.2	5.12
Franklinite	5.0 – 5.22	5.12
Hematite	4.9 – 5.3	5.18
Cuprite	5.7 – 6.15	5.92
Cassiterite	6.8 – 7.1	6.92
Wolframite	7.1 – 7.5	7.32
Sulfides, arsenides		
Sphalerite	3.5 – 4.0	3.75
Malachite	3.9 – 4.03	4.0
Chalcopyrite	4.1 – 4.3	4.2
Stannite	4.3 – 4.52	4.4
Stibnite	4.5 – 4.6	4.6
Pyrrhotite	4.5 – 4.8	4.65
Molybdenite	4.4 – 4.8	4.7
Marcasite	4.7 – 4.9	4.85
Pyrite	4.9 – 5.2	5.0
Bornite	4.9 – 5.4	5.1
Chalcocite	5.5 – 5.8	5.65
Cobaltite	5.8 – 6.3	6.1
Arsenopyrite	5.9 – 6.2	6.1
Bismuththinite	6.5 – 6.7	6.57
Galena	7.4 – 7.6	7.5
Cinnabar	8.0 – 8.2	8.1
Non-metallic minerals		
Petroleum	0.6 – 0.9	—
Ice	0.88 – 0.92	—
Sea Water	1.01 – 1.05	—
Lignite	1.1 – 1.25	1.19
Soft coal	1.2 – 1.5	1.32
Anthracite	1.34 – 1.8	1.50
Chalk	1.53 – 2.6	2.01
Graphite	1.9 – 2.3	2.15
Rock salt	2.1 – 2.6	2.22
Gypsum	2.2 – 2.6	2.35
Kaolinite	2.2 – 2.63	2.53
Orthoclase	2.5 – 2.6	—
Quartz	2.5 – 2.7	2.65
Calcite	2.6 – 2.7	—
Anhydrite	2.29 – 3.0	2.93
Biotite	2.7 – 3.2	2.92
Magnesite	2.9 – 3.12	3.03
Fluorite	3.01 – 3.25	3.14
Barite	4.3 – 4.7	4.47

is not measured *in situ*, although it can be measured by borehole logging tools (see §11.8.3). Density can also be estimated from seismic velocity (§4.2.8a). Often density measurements are made in the laboratory on small outcrop or drill-core samples. However, laboratory results rarely give the true bulk density because the samples may be weathered, fragmented, dehydrated, or altered in the process of being obtained. Consequently, density is often not very well known in specific field situations.

Density data are given in Table 2.2. Sedimentary rocks are usually less dense than igneous and meta-

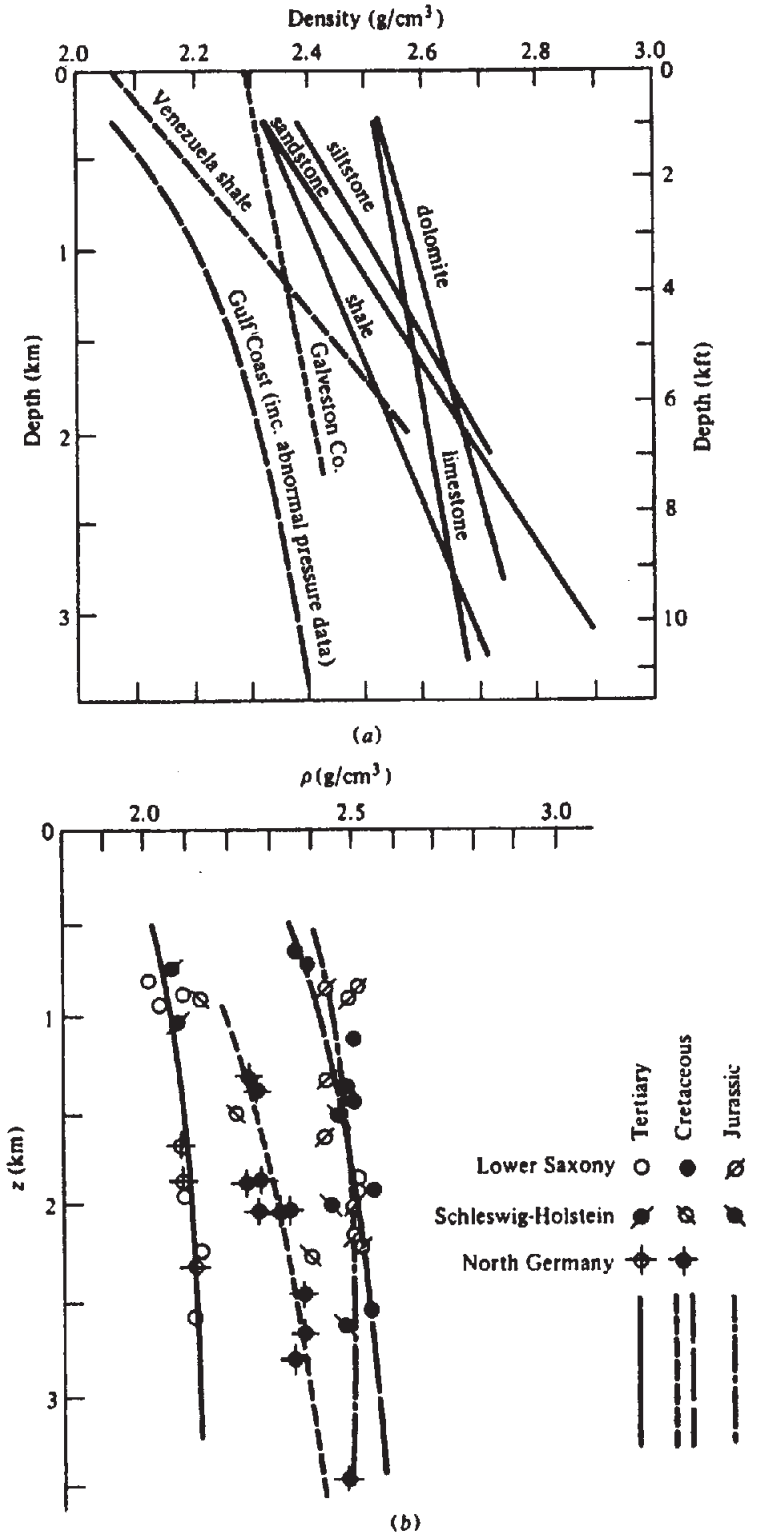

Figure 2.7. Density versus depth. (a) Western Hemisphere data: Venezuelan data from Hedberg (1936), Gulf Coast data from Dickenson (1953), Galveston County data from Bible (1964), and remaining data (Canadian) from Maxant (1980). (b) North Europe data from Hermes (1986).

morphic rocks. The wide range of density of sedimentary rocks is primarily due to variations in porosity. The nature of the pore fluids also affects the bulk density. Sedimentary rock density is also influenced by age, previous history, and depth of burial. Obviously a porous rock will be compacted when buried. In general, density increases with depth (Fig. 2.7) and time. The density contrast between adjacent sedimentary formations in the field is seldom greater than 0.25 g/cm³ (except for the near-surface; §2.7.11).

Although igneous rocks generally are denser than sedimentary rocks, there is considerable overlap. Volcanics, particularly lavas, may have high porosi-